Published in final edited form as:
Biochem Biophys Res Commun. 2010 September 24; 400(3): 340–345. doi:10.1016/j.bbrc.2010.08.059.

Isolation and characterization of the core single-stranded DNA-binding domain of purine-rich element binding protein B (Purβ)

Amy E. Rumora[a], **Ashley N. Steere**[a], **Jon E. Ramsey**[a], **Anna M. Knapp**[a], **Bryan A. Ballif**[c], and **Robert J. Kelm Jr.**[a,b]

[a]Department of Biochemistry, University of Vermont College of Medicine, Burlington, VT 05405

[b]Department of Medicine, University of Vermont College of Medicine, Burlington, VT 05405

[c]Department of Biology and Vermont Genetics Network Proteomics Facility, University of Vermont, Burlington, VT 05405

Abstract

Purβ is a single-stranded nucleic acid-binding protein implicated in the injury-induced repression of genes encoding certain muscle-restricted isoforms of actin and myosin expressed in the heart, skeletal muscle, and vasculature. To better understand how the modular arrangement of the primary sequence of Purβ affects the higher order structure and function of the protein, purified recombinant Purβ was subjected to partial proteolysis in an attempt to identify a well-folded truncation protein that retained purine-rich single-stranded DNA-binding activity. Limited tryptic digestion of Purβ liberated a core ~30 kDa fragment corresponding to residues 29–305 as determined by epitope mapping and mass spectrometry. Size exclusion chromatography indicated that the isolated core fragment retains the ability to self-associate while circular dichroism analysis confirmed that the Purβ core domain is stably folded in the absence of glycine-rich N- and C-terminal sequences. Comparative DNA-binding assays revealed that the isolated core domain interacts with purine-rich *cis*-elements from the smooth muscle α-actin gene with similar specificity but increased affinity compared to full-length Purβ. These findings suggest that the highly conserved modular repeats of Purβ fold to form a core functional domain, which mediates the specific and high affinity binding of the protein to single-stranded DNA.

Keywords

Purβ; PUR repeat; purine-rich element; single-stranded DNA; smooth muscle α-actin

1. Introduction

Purine-rich element binding protein B (Purβ) is a member of a small but highly conserved family of nucleic acid-binding proteins whose signature biochemical feature is preferential interaction with purine-rich single-stranded DNA (ssDNA) or RNA sequences [1]. The founding and most widely studied member of this family, Purα, is involved in many aspects

Address correspondence to: Robert J. Kelm, Jr. University of Vermont Colchester Research Facility 208 South Park Drive Colchester, VT 05446 Tel: 802-656-0329 Fax: 802-656-8969 Robert.Kelm@uvm.edu.

of nucleic acid homeostasis including the regulation of DNA replication, DNA repair, gene transcription, RNA transport, and mRNA translation [2,3]. With respect to gene expression, an ensemble of reports have implicated both Purα and Purβ in the repression of genes encoding smooth, cardiac, and skeletal muscle-associated isoforms of actin and/or myosin in stress-activated fibroblasts, smooth muscle cells, cardiomyocytes, and skeletal myoblasts [4–7]. The key biochemical finding shared by these muscle-related studies is the sequence- and strand-specific interaction of Purα and Purβ with GGN repeat-containing *cis*-elements. In the case of the gene encoding smooth muscle α-actin (SMαA), Purα and Purβ appear to repress transcription by ssDNA-binding and protein-protein interaction mechanisms that limit access of *trans*-activators to canonical double-stranded DNA (dsDNA) target sites in the SMαA 5′-flanking region [4,5,8].

Despite the fact that Purα and Purβ are highly homologous [9] and exhibit comparable ssDNA-binding properties *in vitro* [10], these proteins are not entirely redundant in terms of their transcriptional regulatory properties toward specific muscle genes in different cell types. For example, Purβ displays substantially more repressor activity toward the SMαA promoter than Purα when over-expressed in cultured vascular smooth muscle cells [11]. Moreover, gene knockdown and chromatin immunoprecipitation analyses have pointed to endogenously-expressed Purβ as the more crucial player in SMαA gene repression in mouse embryonic fibroblasts [12,13]. A unique role for Purβ in actin and myosin isoform class switching has also been suggested in the context of cardiac transplant remodeling, heart failure, and skeletal muscle performance [14–16]. Biochemical explanations for the seemingly dominant repressor activity of Purβ have included its preferred binding to certain *trans*-activators [12] and its ability to interact cooperatively with multiple ssDNA-binding sites [17].

Published data on the molecular architecture of Purβ is currently limited to aspects of primary, secondary, and quaternary structure [9,13,18]. The primary sequence of Purβ is characterized by alternating basic/aromatic class I and acidic/leucine-rich class II modules which are highly conserved in Purα [9] and all other known members of the Pur protein family in mammals [1,3]. The recently solved x-ray crystal structure of residues 40 to 185 of *Drosophila melanogaster* (*Dm*) Purα has revealed that the first and second class I and II modules fold into two homologous PUR repeats each with ββββα topology [19]. Moreover, intramolecular interaction between the α-helices of the two PUR repeats forms a ssDNA-binding domain resembling the Whirly class of nucleic acid binding proteins [19]. The case for Purβ adopting a similar core structure is supported by sequence homology [9] and site-directed mutagenesis studies indicating that certain amino acids within this region are critical to the conformational stability and functional activity of the protein [13]. However, Purβ does possess some unique features including two internal glycine/proline-rich stretches, which interrupt the second PUR repeat, and other distinguishing sequence elements near the N- or C-terminal regions of the protein, which may serve to modulate its ssDNA-binding function [10,11]. In this study, we utilized limited proteolysis to probe the structure of recombinant mouse Purβ in solution and to identify a well-folded core domain that mediates specific and high affinity binding of Purβ to ssDNA.

2. Material and methods

2.1. Recombinant Purβ purification

Full-length mouse Purβ was expressed in *E. coli* as an N-terminal 6×His-tagged fusion protein and purified by metal chelate affinity and calibrated size exclusion chromatography (SEC) [18]. Protein purity was assessed by sodium dodecyl sulfate-polyacrylamide gel electrophoresis (SDS-PAGE) under reducing conditions and staining with Coomassie® Brilliant Blue R-250. Absence of nucleic acid in NHis-Purβ preparations was confirmed by

determining the A260/A280 ratio. Protein concentration was calculated based on theoretical molar extinction coefficient for NHis-Purβ at 280 nm of 20,400 M^{-1} cm^{-1}.

2.2. Proteolytic resistance assay

Limited digestion reactions were initiated by the addition of either sequencing- or proteomics-grade trypsin (Roche Applied Science or Sigma-Aldrich) to 3.0 or 5.0 μM solutions of NHis-Purβ at 4°C in buffer consisting of 50 mM sodium phosphate pH 7.5, 300 mM NaCl, 0.5 mM EDTA, and 10 mM β-mercaptoethanol (β-ME). Purβ to enzyme mass ratios were tested at 10:1 and 25:1. Aliquots were removed at 0, 15, 30, 60, 90, or 120 min time points, supplemented with 1% w/v SDS and 5% v/v β-ME, and heated at 95°C for 5 min. Protein fragments were separated by SDS-PAGE (12% or 10% mini-gel) and visualized by Coomassie® Brilliant Blue R-250 staining. Alternatively, fragments were transferred to a polyvinylidine fluoride (PVDF) membrane (Immobilon™-P, Millipore) and probed with polyclonal antibodies against selected Purβ sequences [4], a monoclonal antibody against the N-terminal $RGS(H)_6$ tag (Qiagen), or biotinylated ssDNA (Supplementary Methods). Prestained markers (New England Biolabs or Invitrogen) were used as molecular weight standards on western and southwestern blots. Wide range SigmaMarker™ standards (Sigma-Aldrich) were used on stained gels.

2.3. Purification of the Purβ core tryptic fragment

A 1 mg/ml solution of NHis-Purβ was combined with proteomics grade trypsin at a protein to enzyme ratio of 500:1. After incubating for 6 h on ice, Nα-tosyl-lysine-chloromethylketone and benzamidine were sequentially added to a final concentration of 0.1 mM and 10 mM, respectively. Insoluble material was removed by centrifugation at 2,500 × g for 5 min and the soluble digest was applied to a small column packed with ~2 ml heparin-agarose (Sigma-Aldrich) equilibrated with 20 mM Tris-Cl pH 7.4, 300 mM NaCl, 0.5 mM EDTA, 0.1 mM benzamidine, 0.1 mM phenylmethanesulfonylfluoride, and 10 mM β-ME. Bound protein was eluted by applying a linear gradient of 0.3 M to 2.0 M NaCl in column equilibration buffer. Individual fractions were analyzed by SDS-PAGE to identify those enriched in the core fragment. The concentration of the core fragment in pooled fractions was calculated assuming a molar extinction coefficient at 280 nm of 20,400 M^{-1} cm^{-1}.

2.4. Circular dichroism (CD) spectroscopy

Purified NHis-Purβ or the core fragment were dialyzed into buffers consisting of 10 mM Tris-Cl pH 7.5, 150 mM NaCl, 0.5 mM EDTA, 0.5 mM DTT or 50 mM Tris-Cl pH 7.5, 300 mM NaCl, 0.5 mM EDTA, 0.5 mM TCEP. Data were collected on a Jasco model 815 spectrometer using a 1 mm cuvette at 25°C. Multiple wavelength scans (typically 8) were collected between 260 and 195 or 197 nm at 1 nm intervals. Recorded CD spectra in millidegrees were averaged, corrected for buffer, and then converted into mean residue ellipticity in deg cm^2 $dmol^{-1}$ using the formula,

$$[\theta] = \theta_{obs} / (c \cdot l \cdot n)$$

in which θ_{obs} is observed ellipticity in millidegrees, c is the molar protein concentration, l is the path length of the cuvette in millimeters, and n corresponds to the number of amino acid residues. CD data were analyzed using the K2d algorithm (http://www.embl.de/~andrade/k2d/) [20].

2.5. Intact protein mass spectrometry

Intact proteins were reduced, alkylated using iodoacetamide, and then dialyzed against 50 mM ammonium bicarbonate. Ten μg of each protein was dried separately using a

lyophilizer. Protein was resuspended in 5 μl of 50% acetonitrile (ACN), 2.5% formic acid (FA) and then an additional 15 μl of 2.5% ACN, 2.5% FA for a final concentration of 14.4% ACN, 2.5% FA. Five μl was loaded, using a MicroAS autosampler and Surveryor Pump Plus HPLC (Thermo Electron), on to a nano-ESI microcapillary column with an internal diameter of 100 μm and packed with 12 cm of reverse-phase C4 resin. HPLC solvent A was 2.5% ACN, 0.15% FA. HPLC solvent B was 99.85% ACN, 0.15% FA. After a 15 min isocratic loading in solvent A, proteins were eluted into a LTQ-orbitrap (Thermo Electron) hybrid mass spectrometer using a 20%–80% ACN gradient. Mass measurements were made in the orbitrap at 30,000 resolution.

2.6. DNA-binding assays

An enzyme-linked immunosorbent assay (ELISA) was conducted using synthetic biotinylated ssDNA probes (Table S1) immobilized on StreptaWells (Roche Applied Science) at a concentration of 0.5 nM as previously described [13]. Briefly, ssDNA-coated wells were incubated overnight with 1.0 nM solutions of full-length NHis-Purβ or the core fragment in binding buffer consisting of 20 mM Hepes pH 7.5, 150 mM NaCl, 1.5 mM $MgCl_2$, 0.5 mM DTT, 1.0 μg/ml dT32 with 0.2% w/v BSA and 0.05% v/v Tween® 20. Nucleoprotein complexes were detected by sequentially washing and then incubating the wells with 1) 1.0 μg/ml primary rabbit polyclonal antibody recognizing the Purβ 210–229 epitope [4], 2) 1:8000 dilution of secondary horseradish peroxidase-coupled goat anti-rabbit antibody (Santa Cruz Biotechnology, Inc.), and 3) ABTS chromogenic substrate solution (Millipore).

A competitive colorimetric DNA-binding assay was performed using microtiter wells coated with 20 nM NHis-Purβ plus 5.0 μg/ml BSA carrier as previously described [13]. Briefly, Purβ-coated wells were incubated with 0.5 nM biotinylated PE32-F ssDNA in the presence of selected concentrations of fluid-phase competitor (either full-length NHis-Purβ or the core fragment) diluted in binding buffer. After overnight incubation at 25°C, wells were sequentially washed and incubated with solutions containing ExtrAvidin®-peroxidase diluted 1:2000 followed by ABTS chromogenic substrate (Millipore). In both the direct ELISA and competitive DNA-binding approaches, the peroxidase substrate reaction was quenched by the addition of an equal volume of 1% SDS. Absorbance values at 405 nm were obtained with a 96 well plate reader (Molecular Devices).

3. Results

3.1. Identification of a trypsin-resistant core domain in recombinant Purβ

To assess the extent of protein asymmetry and existence of tertiary folding within Purβ, purified recombinant NHis-Purβ was subjected to limited trypsin digestion at a concentration in which the protein would be predicted to be mostly dimeric [18]. The proteolytic products were then resolved by SDS-PAGE under reducing conditions and visualized by staining with Coomassie Blue (Fig. 1A). At early time points, four prominent bands were observed that included full-length NHis-Purβ and three closely spaced products of trypsin digestion. Prolonged incubation with trypsin up to 2 hours reduced the number of resolved bands to a single major fragment of M_r ~32 kDa (~30 kDa when taking into account the well documented anomalous electrophoretic mobility of Purβ [4,18]). Importantly, a fragment of identical size was also generated in more dilute solutions of Purβ suggesting that a protease-resistant domain is intrinsic to the monomeric form of the protein as well (Fig. 1C).

3.2. Primary structure of the Purβ core tryptic fragment

Tryptic digests of Purβ at various time points were probed by western blotting with antibodies specific for the N-terminal 6×His tag or Purβ peptide sequences spanning amino acids 302–324 or two internal regions from 42–69 and 210–229 (Fig. 1B). Epitope mapping revealed that the core fragment present at the 1 h and 2 h time points nominally contained Purβ sequences from residues 42–69 and 220–229 but was missing the 6×His N-terminus and some C-terminal residues. Southwestern blotting confirmed that the core tryptic fragment retains the ability to bind ssDNA (Fig. 1D). Because tryptic cleavage at R10 and R28 would theoretically produce peptides with N-terminal polyglycine stretches of 9 and 8 residues, we elected to perform targeted LC-MS/MS analysis (as opposed to Edman sequencing) of the core ~30 kDa fragment in comparison to the full-length protein after further in-gel tryptic digestion in order to map the N- and C-terminal boundary peptides of the core fragment. As predicted, a prominent tryptic fragment corresponding to GGGGGGGGPGGEQETQELASK was identified consistent with the N-terminus beginning at G29 (Fig. S1A and Table S2). Other identified peptides indicated that the likely C-terminus of the core fragment extends just beyond the psycho motif to residue 305 (Fig. S1B and Table S2). To validate this conclusion, we also analyzed full-length NHis-Purβ and the core fragment via intact protein ESI-LC-MS and found that the molecular mass of the core fragment does indeed correspond to residues 29–305/306 (Fig. 2).

3.3. Quaternary structure and folding of the Purβ core tryptic fragment

The purified core fragment was subjected to calibrated SEC to determine whether the protein exists as a monomer or dimer at concentrations in the micromolar range. As is evident from the elution profile, the Purβ core fragment overlaps with BSA (~66 kDa), which is consistent with a dimer (Fig. 3A). The relative broadness of the peak, however, is suggestive of a reversible monomer-dimer equilibrium just as previously documented for the full-length protein [18]. Comparative analysis of full-length NHis-Purβ and the core fragment by CD spectrometry indicated that the core fragment is stably folded (Fig. 3B). The modest increase in negative ellipticity between 210 and 222 nm seen with the Purβ core implies a somewhat larger proportion of β-strand and α-helix elements owing to loss of putative random coil-forming N- and C-terminal sequences. Although this feature was observed in both low and high salt buffers, the high glycine content of full-length NHis-Purβ (22%) precluded the computational acquisition of statistically valid numerical values of secondary structure [21].

3.4. DNA-binding properties of the Purβ core trypsin-resistant fragment

Since qualitative southwestern blotting demonstrated the capacity of the core fragment to interact with ssDNA (Fig. 1D), we next studied the ssDNA-binding affinity and specificity of the isolated Purβ core domain in comparison to the full-length protein. A colorimetric, microtiter well-based competition assay was first employed to establish the relative affinity of the core fragment for the SMαA-derived PE32-F element in solution. As shown in Fig. 4A, the competition curve for the core fragment is shifted to the left relative to the full-length protein implying a slightly higher binding affinity for the biotinylated PE32-F probe. In support of this contention, the calculated IC50 values for the full-length protein and the core fragment were 1.3 and 0.5 nM, respectively. These values are consistent with previous estimates of the macroscopic binding affinity of Purβ for this sequence element based on quantitative band-shift and footprinting assays [17].

An ELISA-based assay was used to assess the DNA-binding specificity of the core fragment in comparison to the full-length protein using SMαA-derived *cis*-element probes in both single-stranded and double-stranded configuration [12,13]. These assays were conducted with limiting amounts of purified protein (1.0 nM) and biotinylated DNA (0.5 nM) to

restrict the analysis to high affinity nucleoprotein interactions. As shown in Fig. 4B, the isolated core domain preferentially interacts with purine-rich sense (forward) strands of the PE32 and SPUR32 elements. With respect to the PE32 sequence, individual or combined mutation of the high affinity 3′ and 5′ binding sites and low affinity internal site [17], reduced the interaction of full-length NHis-Purβ and the core tryptic fragment in an analogous fashion (Fig. 4C). To ascertain whether the presence of DNA would affect the susceptibility of the full-length protein to proteolysis, limited tryptic digestion was carried out with solutions containing either polydeoxythymidylate (dT32) as a nonspecific control or PE32-F. As shown in Fig. 4D, although the core fragment was generated in both instances, the presence of equimolar amounts of PE32-F protected the core from complete digestion. These results reinforce the conclusion that the 29–305 region of Purβ constitutes the core ssDNA-binding domain of the protein.

4. Discussion

In an earlier study, we speculated that Purβ may possess some degree of intrinsic structural asymmetry based on hydrodynamic analyses indicating that the Purβ dimer is elongated [18]. Limited proteolysis coupled with the biochemical characterization of peptide fragments resistant to digestion is a classic approach used to identify dimerization regions and/or potential sources of structural asymmetry in DNA-binding proteins [22,23]. Taking into account the modular arrangement of predicted secondary structural elements in Purβ (Fig. S2) and the necessity of all corresponding class I and class II repeats for ssDNA-binding function [11], we hypothesized that these elements might fold in such a way as to protect the central domain of the protein from digestion by trypsin while leaving the putatively more flexible N- and C-termini exposed. Results of our limited proteolysis experiments validated this prediction by identifying a trypsin-resistant, core ssDNA-binding domain extending from residues 29–305. Interestingly, this domain contains the minimal ssDNA/RNA-binding region (residues 37–263) mapped by deletion mutagenesis [11] plus the so-called psycho motif, which is predicted to be α-helical (Fig. S2). Functionally, the Purβ core tryptic fragment mirrors the full-length protein in terms of ssDNA-binding specificity but shows a modestly higher binding affinity presumably due to the absence of an acidic C-terminal tail (Fig. S2). This finding differs from previous results obtained with the 37–263 mutant, which exhibited much weaker ssDNA-binding affinity [11]. Hence, these new data point to a critical role for residues 264–305 in facilitating high affinity binding of Purβ to ssDNA.

These findings are particularly intriguing when considered in conjunction with results of small angle-x-ray scattering measurements and SEC analysis of a *Dm* Purα construct containing PUR repeats I–III [19]. *Dm* Purα I–III, which is analogous to the Purβ core domain described herein, appears to dimerize by virtue of intermolecular interaction between the PUR III repeats (i.e. the third basic/aromatic repeat plus the psycho motif) from each monomer. As a consequence, dimeric Purα adopts an elongated Z-like configuration composed of a central intermolecular PUR domain and two flanking intramolecular PUR domains [19]. If this type of structure is also adopted by the dimeric form of Purβ, then the role of putative α-helix forming residues 264–305 may be to ensure stable self-association of the protein when tethered to ssDNA. Importantly, this type of structural arrangement fits nicely with the cooperative multisite binding mechanism proposed for Purβ interaction with the PE32-F element in the SMαA gene promoter [17]. Multisite contact via individual PUR domains is an attractive model to explain why Purβ interacts preferentially with *cis*-elements containing repeats of consensus and non-consensus PUR elements such as those present in the promoter regions of genes encoding SMαA, α-myosin heavy chain, and β-myosin heavy chain [5–7].

Supplementary Material

Refer to Web version on PubMed Central for supplementary material.

Acknowledgments

The authors thank Shu-Xia Wang for technical assistance and Professor Martin Case for instruction on CD data acquisition.

5. Funding This study was supported by grants NIH R01 HL054281 and AHA 09GRNT2170060 awarded to RJK and the Vermont Genetics Network through NCRR P20 RR016462. AER was supported by NIH training grant T32 HL007594 (Kenneth G. Mann, PI).

References

[1]. Johnson EM. The Pur protein family: clues to function from recent studies on cancer and AIDS. Anticancer Res. 2003; 23:2093–2100. [PubMed: 12894583]

[2]. Bergemann AD, Ma ZW, Johnson EM. Sequence of cDNA comprising the human pur gene and sequence-specific single-stranded-DNA-binding properties of the encoded protein. Mol. Cell. Biol. 1992; 12:5673–5682. [PubMed: 1448097]

[3]. White MK, Johnson EM, Khalili K. Multiple roles for Puralpha in cellular and viral regulation. Cell Cycle. 2009; 8:1–7. [PubMed: 19182532]

[4]. Kelm RJ Jr. Cogan JG, Elder PK, Strauch AR, Getz MJ. Molecular interactions between single-stranded DNA-binding proteins associated with an essential MCAT element in the mouse smooth muscle α-actin promoter. J. Biol. Chem. 1999; 274:14238–14245. [PubMed: 10318844]

[5]. Carlini LE, Getz MJ, Strauch AR, Kelm RJ Jr. Cryptic MCAT enhancer regulation in fibroblasts and smooth muscle cells. Suppression of TEF-1 mediated activation by the single-stranded DNA-binding proteins, Purα, Purβ, and MSY1. J. Biol. Chem. 2002; 277:8682–8692. [PubMed: 11751932]

[6]. Gupta M, Sueblinvong V, Raman J, Jeevanandam V, Gupta MP. Single-stranded DNA-binding proteins PURα and PURβ bind to a purine-rich negative regulatory element of the α-myosin heavy chain gene and control transcriptional and translational regulation of gene expression: Implications in the repression of α myosin heavy chain during heart failure. J. Biol. Chem. 2003; 278:44935–44948. [PubMed: 12933792]

[7]. Ji J, Tsika GL, Rindt H, Schreiber KL, McCarthy JJ, Kelm RJ Jr. Tsika R. Purα and Purβ collaborate with Sp3 to negatively regulate β-myosin heavy chain gene expression during skeletal muscle inactivity. Mol. Cell. Biol. 2007; 27:1531–1543. [PubMed: 17145772]

[8]. Subramanian SV, Polikandriotis JA, Kelm RJ Jr. David JJ, Orosz CG, Strauch AR. Induction of vascular smooth muscle α-actin gene transcription in transforming growth factor β1-activated myofibroblasts mediated by dynamic interplay between the Pur repressor proteins and Sp1/Smad coactivators. Mol. Biol. Cell. 2004; 15:4532–4543. [PubMed: 15282343]

[9]. Kelm RJ Jr. Elder PK, Strauch AR, Getz MJ. Sequence of cDNAs encoding components of vascular actin single-stranded DNA-binding factor 2 establish identity to Purα and Purβ. J. Biol. Chem. 1997; 272:26727–26733. [PubMed: 9334258]

[10]. Wortman MJ, Johnson EM, Bergemann AD. Mechanism of DNA binding and localized strand separation by Purα and comparison with Pur family member, Purβ. Biochim. Biophys. Acta. 2005; 1743:64–78. [PubMed: 15777841]

[11]. Kelm RJ Jr. Wang SX, Polikandriotis JA, Strauch AR. Structure/function analysis of mouse Purβ, a single-stranded DNA-binding repressor of vascular smooth muscle α-actin gene transcription. J. Biol. Chem. 2003; 278:38749–38757. [PubMed: 12874279]

[12]. Knapp AM, Ramsey JE, Wang SX, Godburn KE, Strauch AR, Kelm RJ Jr. Nucleoprotein interactions governing cell type-dependent repression of the mouse smooth muscle α-actin promoter by single-stranded DNA-binding proteins Purα and Purβ. J. Biol. Chem. 2006; 281:7907–7918. [PubMed: 16436378]

[13]. Knapp AM, Ramsey JE, Wang SX, Strauch AR, Kelm RJ Jr. Structure-function analysis of mouse Purβ II: Conformation altering mutations disrupt single-stranded DNA and protein interactions crucial to smooth muscle α-actin gene repression. J. Biol. Chem. 2007; 282:35899–35909. [PubMed: 17906292]

[14]. Subramanian SV, Kelm RJ, Polikandriotis JA, Orosz CG, Strauch AR. Reprogramming of vascular smooth muscle alpha-actin gene expression as an early indicator of dysfunctional remodeling following heart transplant. Cardiovasc. Res. 2002; 54:539–548. [PubMed: 12031699]

[15]. Gupta M, Sueblinvong V, Gupta MP. The single-strand DNA/RNA-binding protein, Purβ, regulates serum response factor (SRF)-mediated cardiac muscle gene expression. Can. J. Physiol. Pharmacol. 2007; 85:349–359. [PubMed: 17612644]

[16]. van Rooij E, Quiat D, Johnson BA, Sutherland LB, Qi X, Richardson JA, Kelm RJ Jr. Olson EN. A family of microRNAs encoded by myosin genes governs myosin expression and muscle performance. Dev. Cell. 2009; 17:662–673. [PubMed: 19922871]

[17]. Ramsey JE, Kelm RJ Jr. Mechanism of strand-specific smooth muscle α-actin enhancer interaction by purine-rich element binding protein B (Purβ). Biochemistry. 2009; 48:6348–6360. [PubMed: 19496623]

[18]. Ramsey JE, Daugherty MA, Kelm RJ Jr. (2007) Hydrodynamic studies on the quaternary structure of recombinant mouse Purβ. J. Biol. Chem. 2007; 282:1552–1560. [PubMed: 17121857]

[19]. Graebsch A, Roche S, Niessing D. X-ray structure of Pur-alpha reveals a Whirly-like fold and an unusual nucleic-acid binding surface. Proc. Natl. Acad. Sci. USA. 2009; 106:18521–18526. [PubMed: 19846792]

[20]. Andrade MA, Chacon P, Merelo JJ, Moran F. Evaluation of secondary structure of proteins from UV circular dichroism spectra using an unsupervised learning neural network. Protein Engineering. 1993; 6:383–390. [PubMed: 8332596]

[21]. Greenfield NJ. Using circular dichroism spectra to estimate protein secondary structure. Nat. Protoc. 2006; 1:2876–2890. [PubMed: 17406547]

[22]. Connaghan-Jones KD, Heneghan AF, Miura MT, Bain DL. Hydrodynamic analysis of the human progesterone receptor A-isoform reveals that self-association occurs in the micromolar range. Biochemistry. 2006; 45:12090–12099. [PubMed: 17002309]

[23]. Finch D, Webb M. Identification and purification of a soluble region in the breast cancer susceptibility protein BRCA2. Protein Expr. Purif. 2005; 40:177–182. [PubMed: 15721786]

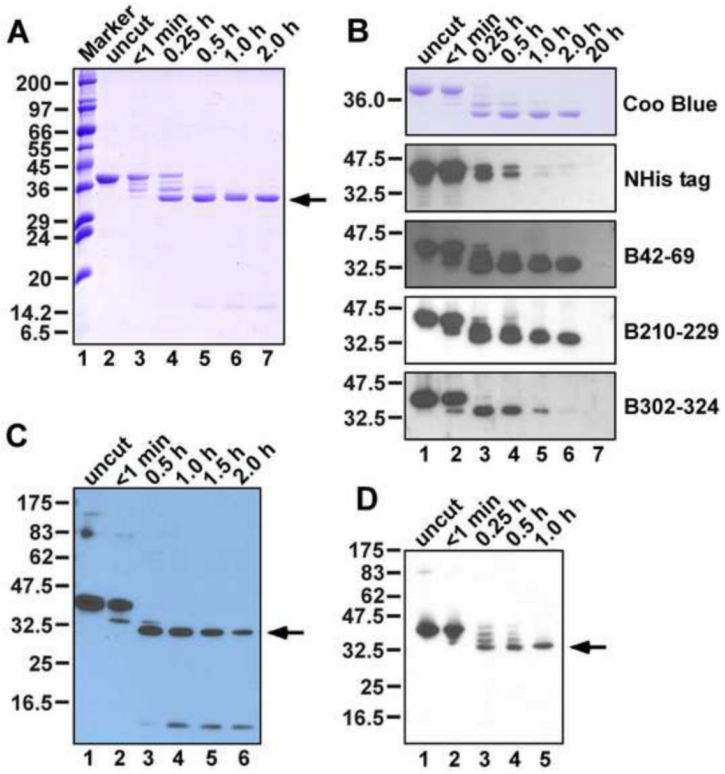

Fig. 1.

Identification of a core trypsin-resistant domain in Purβ. (A) Recombinant NHis-Purβ at 3.0 μM was combined with trypsin at 10:1 mass ratio. Aliquots were removed at the indicated time points. Proteolytic fragments were separated by 12% SDS-PAGE under reducing conditions and visualized by staining with Coomassie® Brilliant Blue. (B) Tryptic digestion mixtures were separated by 10% SDS-PAGE and protein fragments were either stained with Coomassie® Brilliant Blue (Coo Blue) or transferred to a PVDF membrane for immunoblotting with antibodies recognizing the NHis tag or Purβ epitopes B42–69, B210–229, or B302–324. (C) NHis-Purβ at 9.0 nM was incubated with trypsin at a 1:10 mass ratio. Aliquots were removed at the indicated time points and subjected to reducing SDS-PAGE and western blotting using a primary antibody recognizing the 210–229 epitope. (D) A tryptic digest of NHis-Purβ was subjected to southwestern blotting with a SMαA-derived probe. The arrow in panels A, C, and D identifies the core ~30 kDa fragment liberated by trypsin digestion.

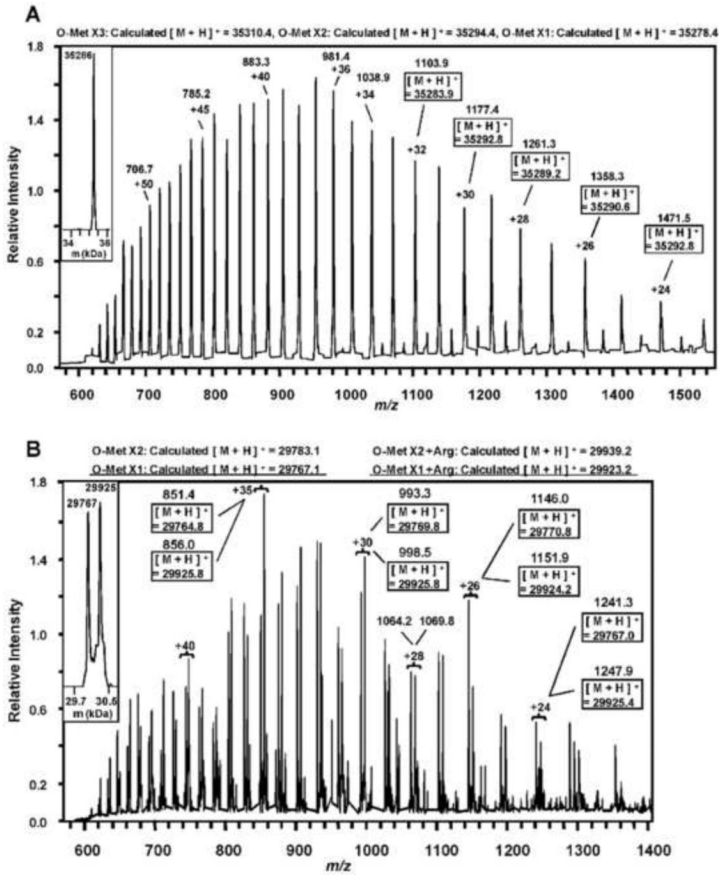

Fig. 2.

Intact protein nano-ESI LC-MS spectra of NHis-Purβ and the core tryptic fragment. A basic deconvolution of the acquired spectra for full-length NHis-Purβ (A) and the core fragment (B) was performed using ProMass (version 25.0.1) using an input *m/z* range of 500–1,550 and an output *m/z* range of 20,000–40,000. The insets show the deconvoluted masses for the proteins based on the composite isotopic envelopes. The spectra are labeled to denote the measured and theoretical (boxed) *m/z* values for a range of charge states. Note for the Purβ core fragment, tryptic digestion could lead to a ragged carboxyl-terminus with or without the protein containing Arg306. This is reflected in the overlapping isotopic envelopes and deconvoluted masses exhibiting mass differences of approximately the mass of arginine (156.1 daltons). The observed and calculated masses for full-length and core Purβ with their respective methionines variably oxidized are indicated above their respective spectra.

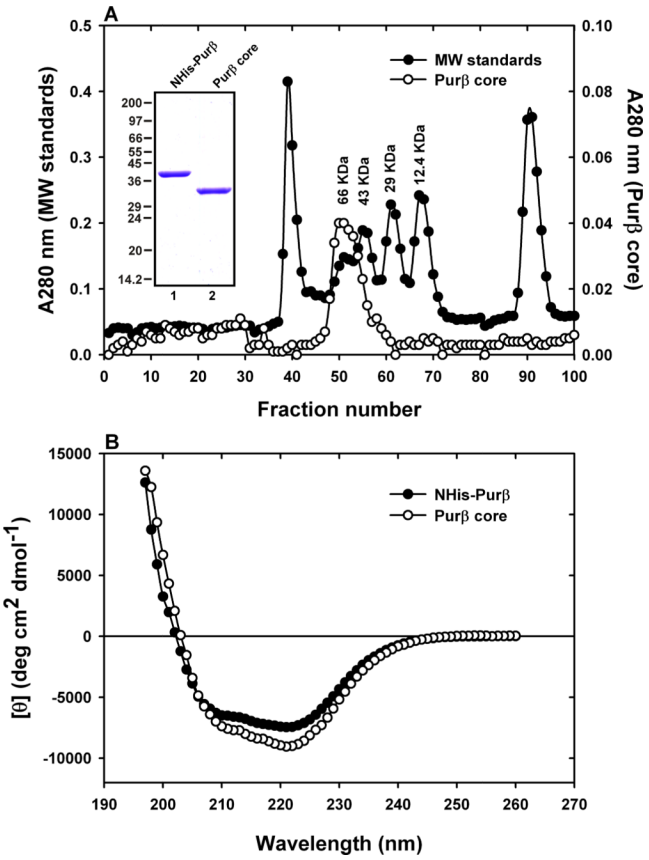

Fig. 3.

Structural analysis of the Purβ core tryptic fragment via SEC and CD spectrometry. (A) A 1.5 × 98-cm column packed with Sephacryl S200 HR resin was calibrated with six different molecular weight standards (●). Resolved peaks corresponding to BSA (66 kDa), ovalbumin (43 kDa), carbonic anhydrase (29 kDa), and cytochrome c (12.4 kDa) are highlighted. In a separate run, the elution of purified Purβ core fragment (0.5 mg loaded) was monitored at 280 nm (◯). Inset, SDS-PAGE analysis of purified proteins. (B) CD scans of full-length NHis-Purβ and the core tryptic fragment were obtained in high salt buffer. The spectrum of the core fragment is consistent with loss of putative N- and C-terminal random coil-forming sequences.

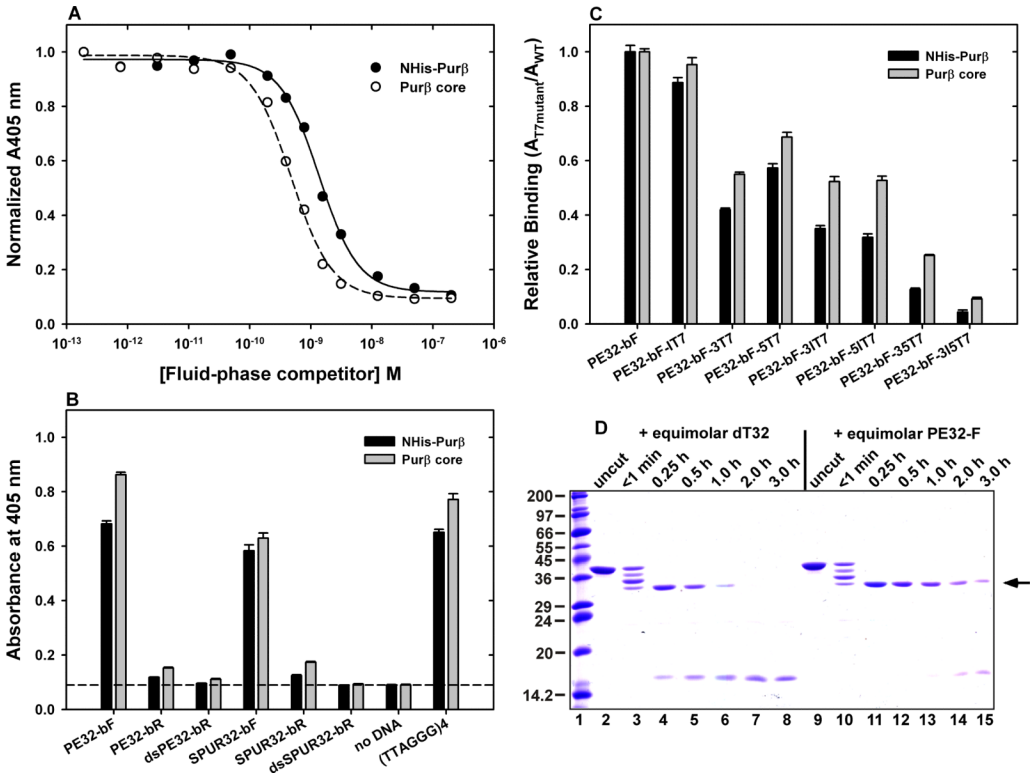

Fig. 4.

Assessment of the ssDNA-binding affinity and specificity of the Purβ core tryptic fragment. (A) A competition assay was conducted with 0.5 nM PE32-bF in the presence of a fixed amount of solid-phase NHis-Purβ and varying amounts of fluid-phase NHis-Purβ (●) or the core fragment (◯). Data points were fit to a four parameter logistic curve using SigmaPlot 9.0 (Systat Software, Inc.). (B, C) ELISAs were performed to compare the binding of NHis-Purβ and the core fragment to StreptaWell-immobilized DNA probes corresponding to wild-type (B) or mutated (C) SMαA *cis*-elements and a telomeric repeat, (TTAGGG)4. (D) Limited tryptic digestion of NHis-Purβ at 5.0 μM was carried out in the presence of equimolar dT32 (lanes 2–8) or PE32-F (lanes 9–15). Lane 1 contains SigmaMarker™ proteins. Arrow shows the core fragment.